Available online at www.sciencedirect.com
ScienceDirect
Journal of Power Sources 172 (2007) 253–264
JOURNAL OF POWER SOURCES
www.elsevier.com/locate/jpowsour

Numerical study on PEMFC's geometrical parameters under different humidifying conditions

Luis Matamoros *, Dieter Brüggemann

Lehrstuhl für Technische Thermodynamik und Transportprozesse, Universität Bayreuth, 95440 Bayreuth, Germany

Received 20 March 2007; received in revised form 31 May 2007; accepted 22 July 2007
Available online 27 July 2007

Abstract

Steady-state and three-dimensional simulations were carried out to study the influences of geometrical parameters on the performance of PEMFC under different hydrating conditions. Flow fields, species transport, transport of water in polymer membrane and movement of liquid water in cathode and anode porous layers were determined, in order to accomplish a complete estimation of ohmic and concentration losses of PEMFC power. The geometrical parameters were thickness of the polymer membrane, cathode catalyst layer as well as gas channel to rib width ratio. Every simulation was made under different relative humidities of inlet flows (50 and 100%) for every change of characteristic length. Results show that the influence of the geometrical parameters on ohmic and concentration losses is of considerable importance. The performance of PEMFC is seriously affected under dehydrating conditions. However, such performance may be considerably improved by using suitable geometrical parameters. Cathode and anode liquid saturation may not only affect the transport of species, but also the polymer electrolyte water content. These results show the importance of simultaneously calculating both the water absorption and desorption through the polymer electrolyte and the liquid saturation in the cathode and anode porous mediums to obtain an actual view of ohmic and concentration losses of the PEMFC performance.

Keywords: PEM fuel cell; Modeling; Simulation; Geometrical parameters; Polymer electrolyte; Saturation

1. Introduction

Modeling and numerical simulation of PEMFC should be aimed for simultaneously calculating the water transfer through the polymer membrane and catalyst layers interface as well as the liquid water saturation in porous mediums. PEMFC's simulations under different hydrating conditions become essential when numerically analyzing the water management. Estimations of concentration and ohmic losses of power under different conditions are important for the optimization of flow fields. Overall losses of power are highly dependant on the water transport and especially on the water content of the polymer membrane, which may be affected by many conditions and parameters.

Many numerical models have been created to account for water management [1–13]. The Wang's review [14] shows a complete description of the most important models published up to now. Recently, Matamoros and Brüggemann [15] simultaneously calculated the water transport in polymer membrane (electro-osmotic drag, back diffusion and water interfacial transfer) and liquid saturation in the cathode porous mediums under different operational conditions. In this former work [15], the authors pointed out the importance of simulating both the polymer electrolyte water transport and the liquid water saturation in order to determine the actual ohmic and concentration losses variations. The condensation of water may not only have an influence on the concentration losses, but also on the ohmic losses by affecting the fraction of water that may be transferred to the polymer membrane. Hence, the water management simulations should include both polymer membrane and two-phase calculations, in order to provide insight into diverse phenomena that can take place when operating the PEMFC under different conditions.

The objective of the present work is to analyze the influences that some geometrical parameters (thickness of polymer membrane, cathode catalyst layer and gas channel to rib width ratio) may have on the water transport and as such on the performance of a straight PEMFC under different hydrating conditions, in

* Corresponding author. Tel.: +49 921 557168; fax: +49 921 557165.
E-mail address: luis.matamoros@uni-bayreuth.de (L. Matamoros).

0378-7753/$ – see front matter © 2007 Elsevier B.V. All rights reserved.
doi:10.1016/j.jpowsour.2007.07.038

Nomenclature

A_{LG}/V_L	gas–liquid interfacial area (m^{-1})
A_{superf}	Pt area per Pt mass ($m^2\,kg^{-1}$)
c_p	volumetric thermal capacity ($J\,kg^{-1}\,K^{-1}$)
C	molar concentration ($kmol\,m^{-3}$)
C_{O_2ref}	oxygen reference molar concentration ($kmol\,m^{-3}$)
C_{O_2s}	oxygen molar concentration at the agglomerate surface ($kmol\,m^{-3}$)
CCL	cathode catalyst layer
CCLT	cathode catalyst layer thickness (m)
CGDLT	cathode gas diffusion layer thickness (m)
D	diffusivity ($m^2\,s^{-1}$)
F	Faraday constant
GCW	gas channel width (m)
i_{oref}	reference exchange current density ($A\,m^{-2}$)
K_p	hydraulic permeability (m^2)
m_{Pt}	Pt mass per volume ($kg\,m^{-3}$)
M	molecular weight ($kg\,kmol^{-1}$)
$\dot{n}_{GLH_2O}$	volumetric condensation rate ($kg\,s^{-1}\,m^{-3}$)
N	molar flux ($kmol\,m^{-2}\,s^{-1}$)
N_{Drag}	electro-osmotic drag factor ($kmol_{H_2O}\,(kmol_{H^+})^{-1}$)
P	pressure (Pa)
PM	polymer membrane
PMT	polymer membrane thickness (m)
r	reaction rate ($kmol\,s^{-1}\,m^{-3}$)
R_{agg}	agglomerate ratio (m)
RH	relative humidity
S	saturation factor
S_ϕ	source term
T	temperature (K)
V	velocity ($m\,s^{-1}$)
x	molar fraction
y	mass fraction

Greek letters

α_c	transfer coefficient cathode side
δ	thickness (m)
ϵ	porosity
η	cathode overpotential (V)
θ	contact angle (rad)
λ	water content ($kmol_{H_2O}\,(kmol_{SO_3^-})^{-1}$)
μ	dynamic viscosity ($kg\,m^{-1}\,s^{-1}$)
ϱ	density ($kg\,m^{-3}$)
σ	surface tension (Nm^{-1})

Subscripts

agg	agglomerate
c	capillary
G	gas
H^+	proton
H_2O	water
i	species i
im	immobile
j	species j
L	liquid
m	mixture
O_2	oxygen
SO_3^-	sulfonate group
V	vapor

order to analyze the diverse phenomena that may dominate electrochemical mechanisms in these systems.

The effects of the parameters, like gas channel and ribs width as well as the porosity of the gas diffusion layers, on the PEMFC performance were recently studied in Refs. [12,13] using CFD modeling. In these works [12,13], isothermal operation and single phase flow were assumed. The interfacial polymer membrane water content was evaluated in Refs. [12,13] by using Springer et al. [16] equilibrium correlation at 30 °C. This means that the diffusion resistance in the non-equilibrium process of water transfer through the polymer membrane interface was not considered. The boundary condition at the polymer membrane interface should be modeled by diffusion in both mediums when using differential modeling. Otherwise the water transfer in and out of the polymer membrane cannot be established. It is important to mention that the equilibrium polymer electrolyte water content at higher temperatures than 30 °C should be estimated, given that the polymer electrolyte is dehydrated by increasing the temperature. The data of Hinatsu et al. [17] at 80 °C can be useful to achieve an estimation of the equilibrium water content of the polymer electrolyte at temperatures between 30 and 80 °C by linear interpolation. When assuming catalyst layers as a surface, ohmic losses in this region are considered as negligible. It is important to model the resistance to the proton flux exerted by the polymer electrolyte contained in the cathode catalyst layer, especially at dehydrating conditions, given that such process may affect the activation potential of the catalyst, and so the sensitivity of the numerical modeling under different conditions may be different. As aforementioned, the present work aims for studying the effects of several geometrical parameters on PEMFC performance, giving special attention to ohmic losses in the polymer membrane and cathode catalyst layer, which highly depend on the water movement in PEMFC. Consequently, the phenomenon like the interfacial water transfer through the polymer membrane boundaries, the change of polymer electrolyte water content at different temperatures, and the change of overpotential in the cathode catalyst layer should be properly accounted for. Therefore, the present work shows the considerable sensitivity of this modeling under different conditions which may be interesting when studying and understanding the electrochemical and transport processes that may dominate the power output of PEMFC using numerical tools.

Even though the concentration losses in the anode side are considered insignificant in the present work, the liquid water saturation in anode porous mediums is included in the simulations, given that this phenomenon may influence the water transfer through the polymer membrane and anode porous medium

interface. In other words, the presence of liquid water in the anode porous mediums affects the anode water balance. Consequently a fraction of water may be either absorbed or desorbed by the polymer membrane, another portion may be condensed and the rest may be disposed by the gas flow in channel. Therefore the overall ohmic losses may be affected by the anode condensation of water, which means that this phenomenon should be taken into account, even though the concentration losses in anode may be considered as negligible.

2. Fundamental equations and source terms

The model is three-dimensional and simultaneously calculates the variables of gas channels, catalyst layers and polymer membrane in a straight PEMFC. As mentioned above, the liquid water saturation is not only estimated in the cathode but also in the anode porous layer to improve the estimation of the polymer membrane water content field. Conservation balances and source terms are showed in Table 1.

Diffusion is assumed to be the primary mechanism of transport in the gas diffusion layers and catalyst layers while the convection is assumed as negligible. The pressure drop in gas channels (source term of momentum in gas channels) is estimated using the Darcy friction factor, consequently the use of coupled pressure–velocity equations was avoided. The source term of the continuity equation can be ignored [18].

Joule heating in polymer membrane, heat produced in cathode reaction and heat produced in condensation–evaporation entropy change are taken into account as source terms of energy S_T. Joule heating S_{T1} in the membrane is calculated by using the proton conductivity in Nafion k_{H^+} and the proton flow. It is important to mention that the energy balance in the polymer membrane was calculated assuming the thermal conductivity as $100\,\mathrm{W\,m^{-1}\,K^{-1}}$ [19]. Heat produced in the cathode reaction is determined using the reaction heat of oxygen reduction $\Delta \mathrm{Hr}_{O_2}$ and reaction rate, which basically consists of heat produced by the entropy change and cathode overpotential [20]. Condensation–evaporation entropy change in cathode porous mediums is estimated using the latent heat of vaporization of water at local temperature H_{LG} and the volumetric condensation rate.

The electrochemical kinetic was determined by using the agglomerate model [21–25]. The electrochemical reaction rate obtained from the agglomerate model is considered as source term of species S_i in catalyst layers. The stoichiometrical factor of every species is derived from the well-known mechanism of reaction in PEM fuel cells. The agglomerate model states that the catalyst layer is a porous medium composed by platinum and carbon particles mixed together with polymer electrolyte. This mixture is defined as spherical agglomerates, which have void spaces between them. In this work, the polymer electrolyte is assumed as Nafion, the water is assumed to be produced in gas phase and condensation could take place in this medium. The anode reaction is assumed to be dominated by the cathode reaction kinetic, and so the reaction rate is finally expressed as

$$r_{H^+} = \frac{3D_{agg}C_{O_2s}(1-\epsilon)}{R_{agg}^2}(\theta R_{agg}\,\coth\theta R_{agg} - 1) \tag{1}$$

The Thiele modulus (θR_{agg}) can be defined as follows:

$$\theta R_{agg} = \sqrt{\frac{m_{Pt}^{v} A_{superf} i_{oref}}{F D_{agg} C_{O_2 ref}}} R_{agg}\,\exp\left(-\frac{\alpha_c F\eta}{2RT}\right) \tag{2}$$

The Henry constant for the dissolution of oxygen in water is used to calculate the concentration at agglomerate surface [26]:

$$C_{O_2 s} = x_{O_2}\frac{P}{101325}\,\exp\left(\frac{666}{T} - 14.1\right) \tag{3}$$

The reference exchange current density (i_{oref}) is calculated by the correlation presented by Wang et al. [25] made from the experimental data [27]:

$$\log(i_{oref}) = 7.507 - \frac{4001}{T} \tag{4}$$

The diffusivity of oxygen in Nafion D_{agg} is calculated from the correlation presented by Marr and Li [23], which is made from experimental data [27]:

$$D_{agg} = \left[-1.07\times10^{-5} + 9.02\times10^{-6}\,\exp\left(\frac{T-273}{106.7}\right)\right]\epsilon^{1.5} \tag{5}$$

It is important to mention that the parameter m_{Pt}^{v} represents the volumetric cathode catalyst loading which consists of the relation between the cathode catalyst loading per area and the

Table 1
Conservation balances and source terms

Balance	Differential expression	Source terms
Momentum	$V\cdot\nabla\varrho V = -\nabla P + \nabla\mu\nabla V + S_V$	$S_V = 0$
Energy	$V\cdot\nabla\varrho c_p T = -\nabla k\nabla T + S_T$	$S_{T1} = \frac{(N_{H^+}F)^2}{k_{H^+}}$; $S_{T2} = \Delta \mathrm{Hr}_{O_2} r_{O_2}$; $S_{T3} = \mathrm{H_{LG}}\dot{n}_{GLH_2O}$
Species	$V\cdot\nabla\varrho y_i = -\nabla D_{i,m}\nabla\varrho y_i + S_i$	$S_i = M_i r_i$; $S_{H_2O} = \dot{n}_{GLH_2O}$
Continuity	$\nabla\varrho V = S_m$	$S_m = 0$
Polymer membrane	$\nabla D_\lambda\nabla\lambda = \frac{M_{SO_3^-}}{\varrho_{SO_3^-}}\frac{dN_{Drag}N_{H^+}}{dx}$	$S_\lambda = 0$
Saturation in porous mediums	$\nabla\frac{\varrho_{H_2O(L)}K_p S^3}{\mu_{H_2O(L)}}\left(\frac{dP_c}{dS}\right)\nabla S = S_s$	$S_s = \dot{n}_{GLH_2O}$

cathode catalyst layer thickness as follows:

$$m_{\mathrm{Pt}}^{\mathrm{v}} = \frac{m_{\mathrm{Pt}}}{\delta_{\mathrm{CCL}}} \tag{6}$$

The product of $m_{\mathrm{Pt}}^{\mathrm{v}} A_{\mathrm{superf}}$ yields the volumetric platinum area, which is coupled with the reference exchange current density on platinum surface i_{oref} to define the current output of the cell without considering the concentration and ohmic losses. The cathode catalyst loading value of $m_{\mathrm{Pt}} = 1.0\,\mathrm{mg\,Pt\,cm^{-2}}$ was arbitrarily chosen as base case, and its performance depends on the surface area value ($A_{\mathrm{superf}} = 250\,\mathrm{cm^2\,Pt\,mg^{-1}\,Pt}$), which was also arbitrarily chosen in the range of 110–1400 $\mathrm{cm^2\,Pt\,mg^{-1}\,Pt}$ according to Marr and Li data [23]. Therefore, the performance of present PEMFC directly depends on these factors that numerically yield moderate and high current densities under diverse conditions.

To account for the voltage losses induced by the Nafion resistance to the transport of protons to active sites, a 1D-expression of Ohm's law is defined to estimate the increase of cathode overpotential in the cathode catalyst layer:

$$k_{\mathrm{H^+}}[(1-\epsilon)\epsilon_{\mathrm{agg}}]^{1.5}\frac{\delta\eta}{\delta x} = N_{\mathrm{H^+}}F \tag{7}$$

where $k_{\mathrm{H^+}}[\Omega^{-1}\,\mathrm{m}^{-1}]$ is the proton conductivity in Nafion expressed as [16]:

$$k_{\mathrm{H^+}} = (0.5139\lambda - 0.3260)\exp\left[1268\left(\frac{1}{303} - \frac{1}{T}\right)\right] \tag{8}$$

Two-phase flow in the cathode porous medium (gas diffusion layer and catalyst layer) is assumed as separated phases. Berning and Djilali [6] proposed a liquid water velocity field considering both convection and capillary forces. In this work the liquid is assumed to flow individually driven by capillary pressure gradients, produced by gradients of liquid saturation and surface tension [4,7], consequently the convection is considered as negligible in porous mediums. The capillary pressure is semi-empirically calculated by means of the Leverett function $J(S)$ for hydrophobic unsaturated porous mediums [7,10]:

$$P_{\mathrm{c}} = \frac{\sigma\cos\theta}{(K_{\mathrm{p}}/\epsilon)^{1/2}}J(S) \tag{9}$$

The Leverett function $J(S)$ for hydrophobic porous mediums is expressed as

$$J(S) = 1.417S - 2.120S^2 + 1.263S^3 \tag{10}$$

where the reduced saturation factor S is as follows:

$$S = \frac{s - s_{\mathrm{im}}}{1 - s_{\mathrm{im}}} \tag{11}$$

Below the saturation value s_{im} (immobile saturation), the water is assumed to be a discontinuous flow pattern, and as such the capillary flow can be assumed as negligible. At the gas channel, the liquid water is disposed either by high convective air flow or by evaporation. Then, the reduced saturation factor is assumed to be zero at the gas channel and gas diffusion layer interface [7].

In order to calculate the water change of phase to establish the saturation factor in porous medium, the condensation kinetic theory is used to determine the volumetric condensation rate $\dot{n}_{\mathrm{GLH_2O}}$ which is expressed as

$$\dot{n}_{\mathrm{GLH_2O}} = K_{\mathrm{GL}}M_{\mathrm{H_2O}}\frac{A_{\mathrm{LG}}}{V_{\mathrm{L}}}\frac{P_{\mathrm{H_2O(G)}} - P_{\mathrm{H_2O}}^{\mathrm{Sat}}}{RT} \tag{12}$$

The factor K_{GL} consists of diffusion terms for the condensation process [7]. The evaporation was assumed to be the inverse of the condensation process. The gas–liquid interfacial area $A_{\mathrm{LG}}/V_{\mathrm{L}}$ was arbitrarily assumed as constant. It is important to mention that the condensation and evaporation process in porous mediums is considered as additional source term for water gas balance (Table 1: species balance).

To calculate fuel cell potential, the cathode overpotential and polymer membrane voltage loss are subtracted from the equilibrium potential. The voltage loss produced by bipolar plates and contact resistance between gas channel ribs and gas diffusion layers was assumed as negligible:

$$E = 1.23 - 9\times10^{-4}(T - 298) + \frac{2.3RT}{4F}\log(P_{\mathrm{H_2}}^2 P_{\mathrm{O_2}}) - \eta - \frac{i}{k_{\mathrm{H^+}}} \tag{13}$$

2.1. Transport properties

Gases are assumed as ideal. Dynamic viscosity is determined using the kinetic theory of gases.

In order to consider the influence of porous medium on the conductive transport, the following correction factors were used for catalyst layers and gas diffusion layers, respectively [28]:

$$f(\epsilon) = \epsilon^{1.5} \tag{14}$$

$$f(\epsilon) = \epsilon\left(\frac{\epsilon - \epsilon_\beta}{1 - \epsilon_\beta}\right)^{\alpha} \tag{15}$$

The factor ϵ_β is considered as 0.11 and α is 0.527 for in-plane diffusion and 0.785 for cross-plane diffusion [7].

Thermal conductivities are expressed as an average between conductivities of phases involved in each infinitesimal element of the system:

$$k = k_{\mathrm{S}}f(1-\epsilon) + k_{\mathrm{G}}f(\epsilon)(1-s) + k_{\mathrm{L}}f(\epsilon)s \tag{16}$$

Volumetric thermal capacity is also regarded as an average between phases. Consequently, thermal equilibrium between phases is assumed:

$$c_{\mathrm{p}} = c_{\mathrm{pS}}(1-\epsilon) + c_{\mathrm{pG}}\epsilon(1-s) + c_{\mathrm{pL}}\epsilon s \tag{17}$$

Mixture diffusivity was approximated by the mixture rule [29]:

$$D_{i,\mathrm{m}} = \frac{\sum_{i=1,i\neq j}^{n} x_i M_i}{\sum_{i=1}^{n} x_i M_i \sum_{i=1,i\neq j}^{n} x_i/D_{i,j}} \tag{18}$$

Binary diffusivities were calculated using the following correlation for gases at low density [29]:

$$\frac{PD_{i,j}}{(P_{ci}P_{cj})^{1/3}(T_{ci}T_{cj})^{5/12}((1/M_i)+(1/M_j))^{1/2}} = a\left(\frac{T}{\sqrt{T_{ci}T_{cj}}}\right)^{b} \quad (19)$$

In this equation, a and b are constants. If the mixture diffusivity is calculated for a porous medium, Eqs. (14) and (15) are used to account for the effect of porosity and tortuosity of the catalyst layer and gas diffusion layer, respectively. The effect of liquid water saturation is accounted for by using a normalized function $f(s) = (1-s)^{1.5}$. Therefore, the final form of the diffusivity is

$$D_{i,\text{m-corrected}} = D_{i,\text{m}} f(\epsilon) f(s) \quad (20)$$

For the polymer electrolyte, the electro-osmotic drag coefficient N_{Drag} was calculated at 30 and 80 °C using the empirical data for Nafion from Springer et al. [16] and Neubrand [30], respectively. Concerning the diffusion coefficient of water in the polymer electrolyte, the following approach was made from the data of Zawodzinski et al. [31] (30 °C) and Neubrand [30] (80 °C) to determine the value of this property:

$$D_\lambda = 1.5 \times 10^{-7}\lambda\, \mathrm{e}^{-2436/T} \quad (21)$$

2.2. Boundary conditions

In order to determine the interfacial water transfer between the cathode and anode porous mediums and the polymer membrane, the difference between the bulk concentrations of water in each phase and the equilibrium concentrations of water at the interface was used as driving force of absorption and desorption of water by the polymer electrolyte. The convective mass transfer is neglected, and so the water exchange is expressed in terms of the molar fraction of each phase (Y_i and X_i) and the mixture diffusivity of species i by each phase ($D_{i,\text{m1}}$ and $D_{i,\text{m2}}$):

$$\varrho_1 D_{i,\text{m1}} \frac{X_i - X_i^*}{M_1 \Delta x_1} = \varrho_2 D_{i,\text{m2}} \frac{Y_i^* - Y_i}{M_2 \Delta x_2} \quad (22)$$

The equilibrium data from Springer et al. [16] at 30 °C and from Hinatsu et al. [17] at 80 °C were used to complete this interfacial mass transfer model by relating the molar fraction of water of each phase at the interface (Y_i^* and X_i^*). The interfacial polymer membrane water content at different temperatures is calculated by linear interpolation. The water uptake from vapor phase is likely to mostly hydrate the polymer membrane [31], given that the catalyst layer and gas diffusion layer must be almost flooded to account for a significant liquid water uptake.

Considering that ohmic losses are also calculated in the cathode catalyst layer, the water content of the polymer electrolyte contained in this region is assumed to be uniform and equal to the calculated interfacial water content of polymer membrane. Hence, the water content balance (Table 1) is only used in polymer membrane. Using a model for the absorption and desorption of water in the catalyst layer would be highly difficult, given the complexity of the porous structure of this region. Therefore, the water transfer in and out of the polymer electrolyte is assumed to take place only at the polymer membrane–catalyst layer interface which is considered as a plane.

3. Results and discussion

As mentioned above, the concentration and ohmic losses may either highly or slightly depend on the geometrical parameters of PEMFC. The geometrical parameters can be of high importance when simulating such systems, consequently their effects should not be taken for granted when either analyzing the water management or validating data. Values of thickness of polymer membrane, cathode catalyst layer and gas channel to rib width ratio were varied between low and high magnitudes under different humidifying conditions (50 and 100%). The effect of gas diffusion layers permeability is also simulated in order to analyze the behavior of concentration losses caused by liquid saturation when using gas diffusion layers with different properties. Results are mostly presented as transversal averages along the gas channel, given that two- and three-dimensional displays are not practical to make comparisons. Power density distributions represent the product of current density and cell potential distributions. It is important to mention that the local ohmic losses in the polymer membrane and the overpotential are used to estimate the cell potential distribution. Results are also showed as polarization curves, in order to enhance the presentation of power and current density distributions.

Table 2 summarizes the base geometrical and electrochemical parameters arbitrarily used in this work. Both cell potential and current density were output variables in simulations. The cathode overpotential is used as controlling input variable, given that both cell potential and current density mainly depend on the concentration and ohmic losses fields in the polymer membrane and cathode catalyst layer. Therefore, their averages and fields

Table 2
Geometrical and electrochemical parameters

Description	Value
Channel height (m)	0.0004
Channel width (m)	0.001
Channel length (m)	0.10
Channel rib (m)	0.0002
Gas diffusion layer thickness (m)	0.0001
Gas diffusion layer porosity	0.5
Catalyst layer thickness (m)	0.00001
Catalyst layer porosity	0.4
Polymer membrane thickness (m)	0.0001
Pt loading (mg Pt cm^{-2})	1
Pt surface area (cm^2 Pt g^{-1} Pt)	250,000
Agglomerate porosity	0.2
Agglomerate radii (cm)	0.00001
Inlet cathode volumetric flow (m^3 s^{-1})	0.000001
Inlet anode volumetric flow (m^3 s^{-1})	0.0000005
Inlet cathode flow temperature (K)	353.0
Inlet anode flow temperature (K)	353.0
Inlet cathode flow pressure (Pa)	300,000.0
Inlet anode flow pressure (Pa)	300,000.0

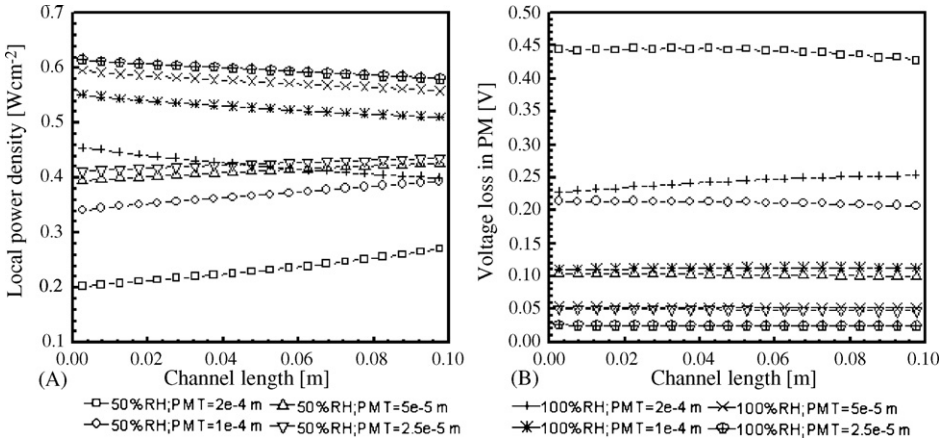

Fig. 1. (A) Average along-channel power density and (B) voltage loss in polymer membrane for different polymer membrane thickness and inlet flow relative humidities.

are known at end of every simulation. The base value of cathode overpotential at the interface cathode catalyst layer–polymer membrane was kept constant at 0.760 V (when calculating distributions of power and current densities) using the electrochemical parameters arbitrarily chosen in this work. This value represents the reaction resistances in the cathode electrode without considering the concentration and ohmic losses [20] (mainly a property of platinum and external circuit resistances). Therefore, cathode overpotential is assumed constant at 0.760 V for every case (except for the polarization curves), in order to obtain high numerical PEMFC output. Such input data configuration was considered suitable to achieve objectives of the present work. Otherwise, a trial-and-error procedure would be necessary to achieve results at constant either current density or cell potential which would not be practical when considering both cell potential and current density as output fields. Inlet flows, pressures and temperatures were kept constant. The cathode inlet flow is three times higher than the necessary flow to produce 1.0 A cm^{-2}. Hence, the concentration losses by oxygen depletion are considerably reduced. Each geometrical parameter was varied at constant inlet relative humidity. Afterwards, the same procedure is repeated but using a different inlet relative humidity. Values of inlet relative humidity were 50 and 100%. Even though the stoichiometry may vary for different inlet relative humidities, its change is assumed as negligible in most of the cases given the excess of reactants.

3.1. Variation of polymer membrane thickness

Polymer membrane thickness is an important parameter to study, due to its influence on the ohmic losses by proton flux resistance from anode to cathode. The proton conductivity may be highly affected by the water content of polymer membrane, and as such ohmic losses in this region depend not only on the proton flux and length of resistance, but also on the interfacial water transfer through the polymer membrane during operation. As well the thickness of polymer membrane is an important length in the process of hydration, given that it proportionally defines the amount of water to be transferred to increase the water content, consequently its magnitude may have a nonlinear influence on ohmic losses and as such on the performance of PEMFC.

Fig. 1 shows averages of the along-channel power density and ohmic losses in the polymer membrane for different PMT using 50 and 100% of RH in both cathode and anode inlet flows. It can be observed in Fig. 1(A) the influence of RH of inlet flows on power density. The magnitudes of power density are lower at 50% RH in comparison to the 100% RH values; given that ohmic losses in CCL and PM considerably increase for lower RH as shown in Fig. 1(B). The PEMFC power density improves for thinner membranes, given that the ohmic losses in PM are considerably decreased (Fig. 1(B)) for both RH cases. The ohmic losses at 50% RH seem to be uniform along the gas channel, on account of the compensation between the gradual humidification of polymer membrane and the increase of current density along the gas channel. This increase of current and power density is produced by the decrease of ohmic losses in CCL and PM as a result of the humidification of the polymer electrolyte. Under fully humidifying conditions, the lack of oxygen depletion causes uniform polymer membrane voltage loss along the gas channel. In conclusion, it can be seen in Fig. 1 that the ohmic losses can be considerably reduced when using membranes thinner than 50 μm for both 50 and 100% RH.

Fig. 2 shows the polarization curves for different polymer membrane thickness at 50 and 100% RH, in order to improve the former observations. The ohmic losses seem to be considerably diminished at 50% when using thin polymer membrane (e.g. 25 and 50 μm). The differences between 100% RH (fully humidifying conditions) and 50% (dehydrating condition) are not dramatical when using such thin membranes. Therefore, suitable operation can be achieved under such conditions. These results show the importance of numerically taking into account every effect that may influence the water transport, in order to determine the actual ohmic and concentration losses and reliably predict the actual PEMFC behaviors.

Fig. 3 shows 100 μm thick polymer membrane water content fields (base case) at different inlet flow RH (50 and 100% RH, respectively) to provide insight into water distributions in the polymer membrane. It can be seen in Fig. 3(A) that the polymer membrane is considerably dried at the entrance of the gas

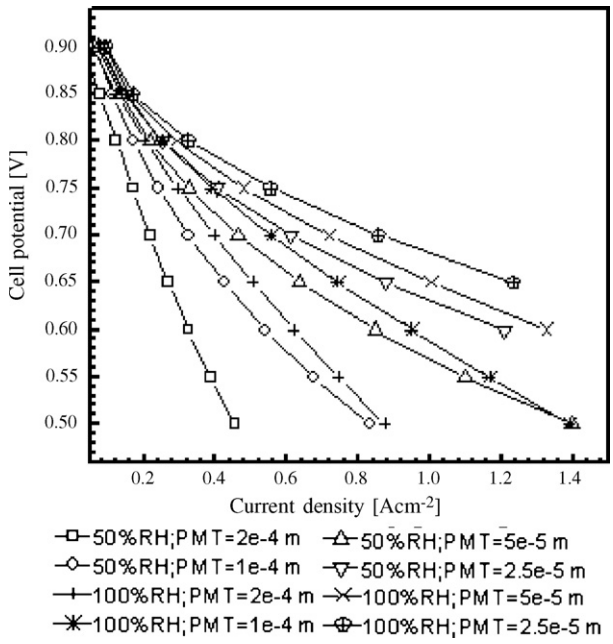

Fig. 2. Cell voltage vs. average current density for different polymer membrane thickness and inlet flow relative humidities.

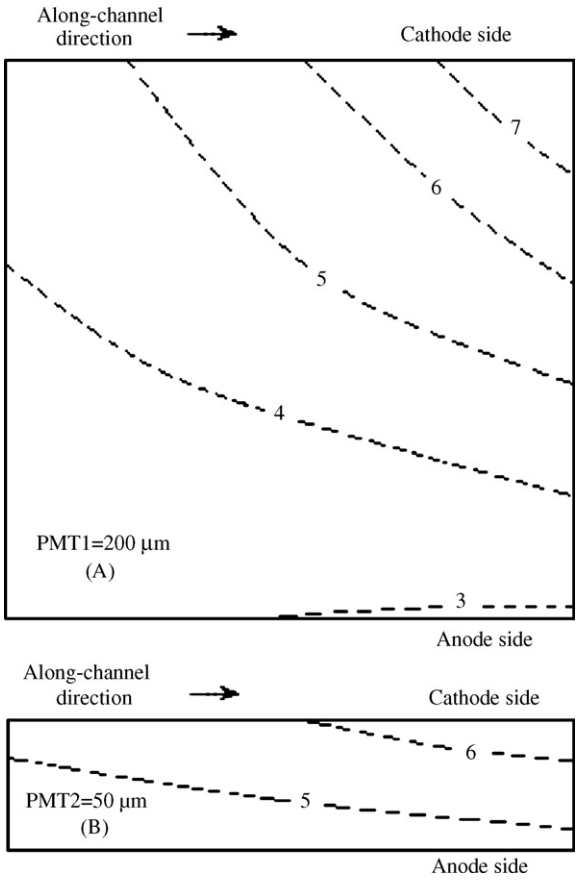

Fig. 4. Polymer membrane water content [$kmol_{H_2O}\ (kmol_{SO_3^-})^{-1}$] at 50% RH (A) PMT = 200 μm and (B) PMT = 50 μm.

channel when operating at 50% RH. The ohmic losses reduce the cathode reaction rate and so the water production is not high enough to effectively increase the along-channel water content (approximately from 4 to 7). At 100% RH (Fig. 3(B)), the water content is almost uniform along the gas channel. Even though the water fraction increases along the gas channel, the water content tends to be slightly higher at the entrance as product of the higher cathode reaction rate in this area. This behavior means that most of the water is more likely to be disposed by the gas and liquid phase than to be transferred to the polymer electrolyte under fully humidifying conditions. Therefore the polymer membrane water content may be almost uniform along the gas channel under fully humidifying conditions as a result of the water saturation in the control volume (activity 1). The electro-osmotic drag tends to dry the anode side of PM especially at 50% RH. However, fully humidifying conditions in the anode inlet flow (in case B) and the back diffusion contribute to keep water content of PM in anode side.

Back diffusion is an important factor that may be affected by the polymer membrane thickness. Hence, the polymer membrane thickness is a parameter that may nonlinearly affect the performance of PEMFC. Fig. 4 shows two contours of water content along the gas channel at 50% RH, in order to provide insights to this factor for PMT (A) 200 μm and (B) 50 μm. Average current density is 0.8 A cm^{-2} for both Fig. 4(A) and (B). As it can be seen in Fig. 4(A), the water content considerably diminishes from cathode to anode as a product of the electro-osmotic drag and the long path for diffusion of water molecules from cathode to anode side. This effect is considerably decreased for

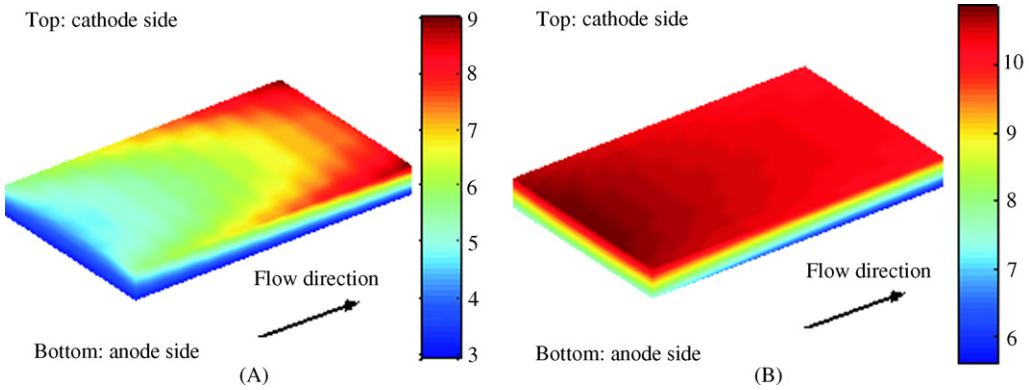

Fig. 3. Polymer membrane water content field [$kmol_{H_2O}\ (kmol_{SO_3^-})^{-1}$] at different inlet flow relative humidities A (50%) and B (100% RH).

thinner membranes, given that back diffusion becomes important in comparison to the electro-osmotic drag, as a product of the shorter path from cathode to anode side (Fig. 4(B)). Fig. 4 shows the high negative effect of the polymer membrane thickness over back diffusion and as such over ohmic losses in PEMFC.

3.2. Variation of cathode catalyst layer thickness

Catalyst layer thickness defines the length for the proton transport through the polymer electrolyte to active sites in the cathode. Ohmic losses in this region depend directly on this parameter. Dehydrating conditions may affect the cathode reaction rate for diverse CCLT. For these reasons the catalyst layer thickness is varied maintaining the catalyst loading per area (1.0 mg Pt cm^{-2}) constant under different humidifying conditions. Even though, the change of catalyst layer thickness causes a variation of catalyst concentration, the total mass of catalysator in the system remains constant.

Fig. 5 shows averages of the along-channel current density for different CCLT using 50 and 100% of RH in both cathode and anode inlet flows. As shown in Fig. 5, ohmic losses in CCL considerably decreases for thinner CCLT. Thinner catalyst layers enhance cathode reaction rate diminishing resistance to transport of proton to reactive sites. Therefore, thin CCLT favors higher current densities, consequently the performance of PEMFC is increased. This enhancement is more important at dehydrating conditions (50% RH). As it can also be seen in Fig. 5, current density is considerably improved for the two thinnest CCL at 50% RH, given that current density distributions are considerably similar at 50 and 100% RH. Hence, ohmic losses in CCL could be considered insignificant for these values. It is important to mention that the slight difference of current density observed for the thinnest CCL is a product of the increase of stoichiometry caused by higher oxygen concentration at 50% RH. However,

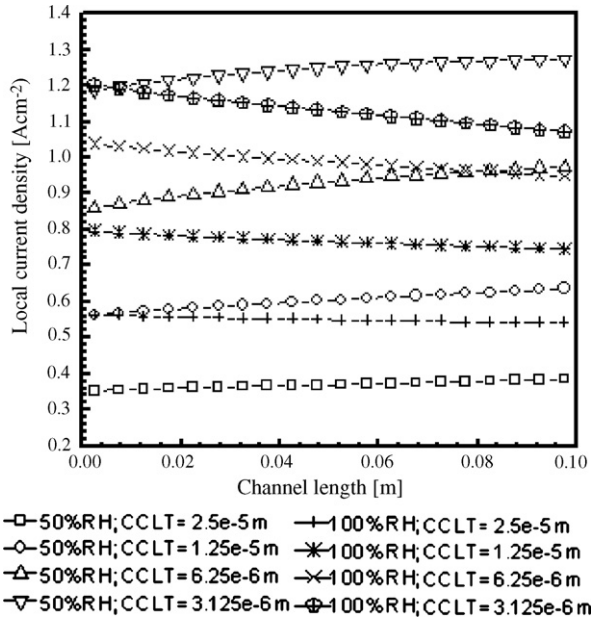

Fig. 5. Average along-channel current density for different cathode catalyst layer thickness and inlet flow relative humidities.

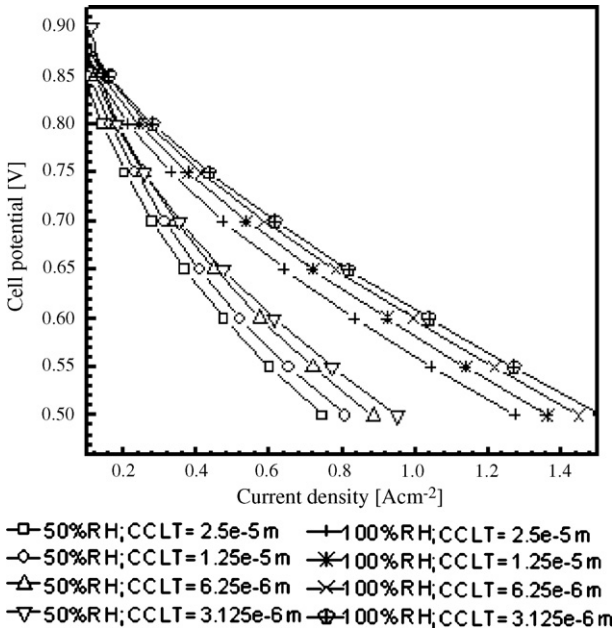

Fig. 6. Cell voltage vs. average current density for different cathode catalyst layer thickness and inlet flow relative humidities.

this observation do not change the fact that ohmic losses are rather small for thinner CCL than 6.25 μm.

Polarization curves were built to show the whole performance of PEMFC (ohmic losses in CCL and PM) for different CCLT at 50 and 100% RH (Fig. 6) and to complete the former observations. As shown in Fig. 6, ohmic losses in CCL are considerably reduced when using thinner electrodes (less than 6.25 μm) at different RH which is in agreement with former observations (Fig. 5). Given that the polarization curves of the two thinnest CCL almost overlap for both RH, it can be concluded that ohmic losses in CCL may be considered as negligible for these values. Therefore, the difference of performance observed in Fig. 6 at different RH is mostly caused by ohmic losses in polymer membrane (base case: 100 μm).

These results show the importance of including CCLT in simulation of PEMFC, even at 100% RH. CCL should be considered as an active volume and not as an active surface, in order to account for ohmic losses caused by polymer contained in this region. Considering CCL as a volume would enhance analyzes concerning PEMFC optimization.

3.3. Variation of gas diffusion layer permeability

Gas diffusion layer permeability is an important parameter that may considerably affect PEMFC performance under fully humidifying conditions. In case the gas diffusion layer permeability is small, water saturation may considerably increase and so power density may be affected by concentration losses caused by resistance to reactant transport to active sites. In numerical terms, this factor dominates the magnitude of saturation by controlling the capillary flow to be disposed to the gas channels.

Fig. 7 (A) and (B) shows the effect of gas diffusion layer permeability on power density (polarizations) and water saturation, respectively. The performance of PEMFC considerably

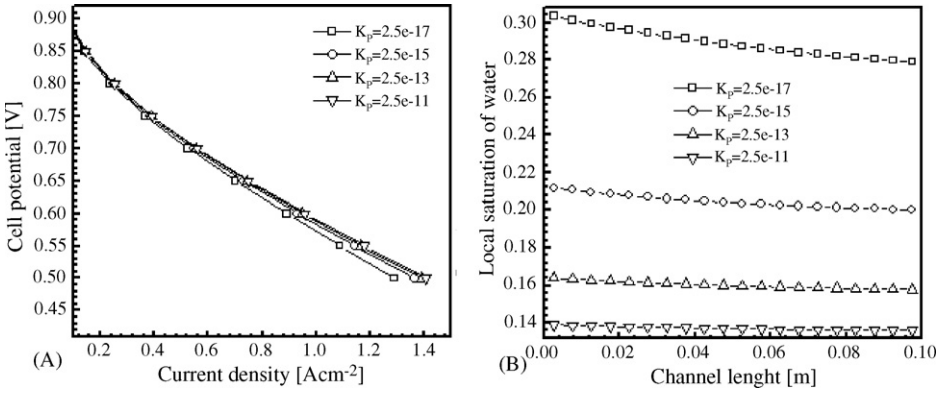

Fig. 7. (A) Cell voltage and average current density and (B) water saturation assuming different cathode permeabilities.

decreases when permeability is low (Fig. 7(A)), given the considerable increase of concentration losses produced by the liquid saturation (Fig. 7(B)). The porosity of gas diffusion layer is kept constant, consequently the behavior observed in Fig. 7 is only caused by changes of the tortuosity of the path for disposal of liquid water. The power density tends to be constant for permeabilities higher than $2.5e{-}15\,m^2$ under high current densities, which means that the saturation is considerably controlled over this value (less than 0.2). These results show how the PEMFC performance may be affected by the liquid saturation and the importance of two-phase flow simulation to reduce the concentration losses caused by the water condensation.

3.4. Variation of cathode gas channel width

Gas channel width represents a characteristic length perpendicular to former lengths. The relation between gas channel and rib width may be of importance, given that the reactants flow through the gas channel and electrons flow through the ribs. Therefore, both lengths are highly important to be considered when analyzing the concentration and ohmic losses. However, the resistance to electron transport through ribs is assumed as negligible in this work.

Gas channel to rib width ratio is varied from 5.0 to 1.0, in order to analyze the behavior of the concentration losses under these conditions. As shown in Fig. 8, the polarization curves overlap for 50% RH. Hence, the effect of GCW is rather small at 50% RH, provided that the ohmic losses dominate over concentration losses induced by narrow gas channel, and so the oxygen diffusion accomplishes to supply the reactant demand under such low cathode reaction rates. Oxygen diffusion is also more effective, given the higher oxygen concentration at dehydrating conditions. The concentration losses at 100% RH increase in comparison to ohmic losses. The increment of humidifying conditions decreases the negative effect of polymer electrolyte proton resistance and as such the cathode reaction rate is favored. Under these conditions, the intensity of reaction is higher and as such is the demand of reactants. To satisfy this demand, the reactant transport must be effective, but the characteristics length like channel width may exert control over the mass transfer. For these reasons the polarizations show slight differences for diverse GCW at 100% RH where the wider gas channels tend to enhance the performance of PEMFC by increasing the area for diffusion of species. As seen in Fig. 8, effect of gas channel width may only be important at high current densities under fully humidifying conditions, given the importance of diffusional control under these conditions. Otherwise, the effect of this parameter can be ignored.

Liquid saturation may not play an important role in these former observations. Fig. 9 shows along-channel distributions of water saturation for different GCW at 100% RH. As it can be seen in Fig. 9, wider channels tend to diminish the saturation in porous mediums, which is a result of major elimination of liquid water by capillary flow. However, the change of water saturation for different GCW may be considered as negligible when analyzing the effect of the gas channel width on PEMFC performance. Under conditions favoring liquid accumulation in gas diffusion layer, gas channel width may play a more important role. As seen in former section, liquid saturation is likely to be highly governed by parameters like the permeability of gas diffusion layer. Liquid saturation is also dominated by the

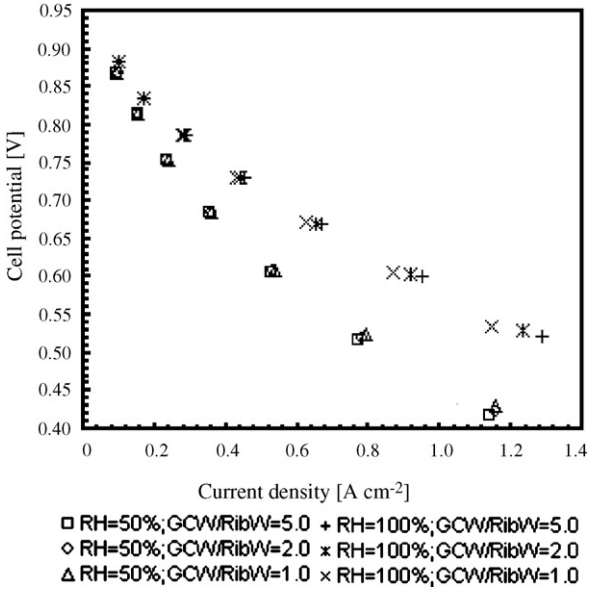

Fig. 8. Average along-channel current density for different gas channel width and inlet flow relative humidities.

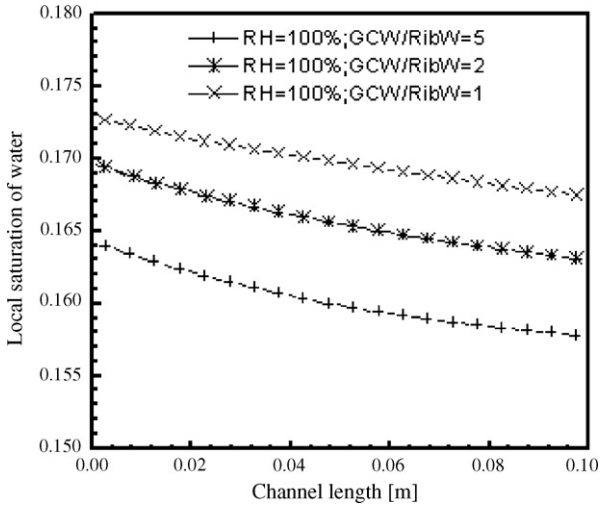

Fig. 9. Average along-channel water saturation for different gas channel width.

hydrophobicity of the gas diffusion medium, which is assumed optimal in this work ($\theta \simeq 110$).

3.5. Effect of ohmic losses on temperature and saturation distributions

Temperature distributions are mostly affected by distributions of ohmic losses in PEMFC. If ohmic losses were low and almost uniform along the gas channel, the system could be assumed as isothermal. As seen before, ohmic losses play an important role for thick polymer membranes, whose effect is considerably decreased when using thinner membranes. Given that the optimal configuration of geometrical parameters considerably reduces the overall ohmic losses even at high current densities and dehydrating conditions, isothermal operation may be assumed in most cases. Temperature distribution may play an important role in a system with serious ohmic losses (e.g. thick membranes greater than 50 μm). Fig. 10 shows temperature and saturation contours for two different polymer membrane thickness ((A and B) 200 μm and (C and D) 50 μm, respectively) when operating at 100% RH, in order to determine the importance of temperature distributions caused by ohmic losses under fully humidifying conditions. The heat is mostly produced by the overpotential at cathode catalyst layer and the Joule heating in the polymer membrane. Therefore, the temperature in gas diffusion layer is likely to show the same tendency as the local current density. In this case temperature distributions are almost uniform as a result of the high convection at gas channel–gas diffusion layer interface and low ohmic losses under fully humidifying conditions (Fig. 10). However, the effect of Joule heating in polymer membrane on temperature and saturation distribution can be observed in Fig. 10. Temperature increases for thicker membranes as a product of higher Joule heating and diminishes along the gas channel due to the gradual reduction of cathode reaction rate (Fig. 10(A)). In direction from polymer membrane to gas channel, the temperature is almost uniform due to the small path to dispose the excess of heat to the gas channel flow. Due to the small residence time of the gas flow, the gas channel temperature may considered uniform, and so the temperature in the along-channel direction shows the decreasing tendency observed in Fig. 10(A). Water saturation basically depends on water activity and temperature. At the gas channel entrance where temperature is higher, water saturation shows an increasing tendency related to the water production in cathode and decrease of temperature along the gas channel (Fig. 10(B)). However, the water saturation reaches a maximum and starts diminishing as a result of the lack of water production. As shown in Fig. 10(C) and (D), the temperature is almost uniform along the gas channel (Fig. 10(C)) and only a slight decrease of water saturation along the gas channel is observed (Fig. 10(D)). As seen in Fig. 10(B) and (D), cathode water saturation is highly dominated by capillary flow and values do not overcome the magnitude of 0.2, given the high permeability of

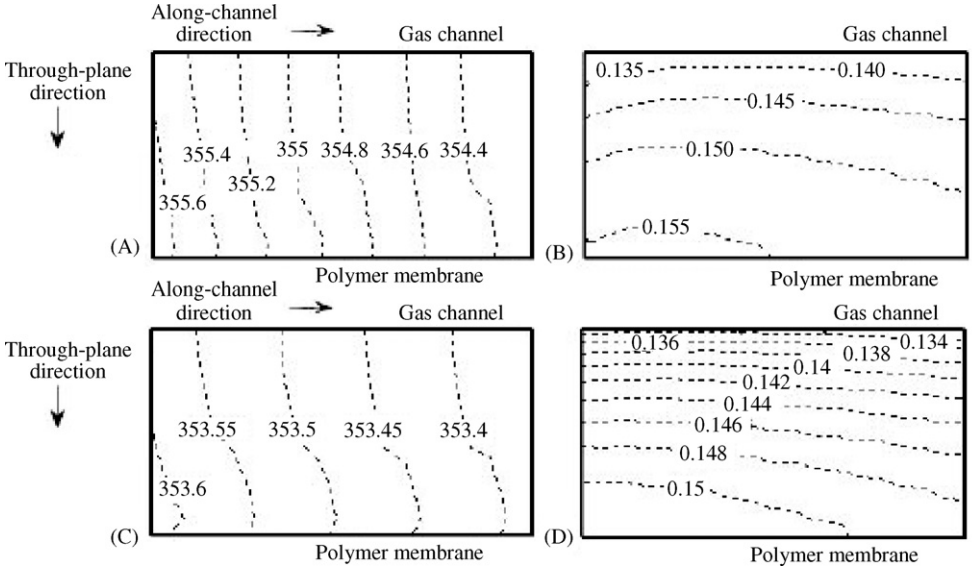

Fig. 10. Through-plane and along-channel distributions of temperature and liquid saturation (A and B) PMT = 200 μm and (C and D) PMT = 50 μm under fully humidifying conditions (100% RH).

base case (1e−13 m^2). Behavior of temperature distributions at 50% RH is assumed to be similar to the case of 100% RH, except for the case of thick membranes where ohmic losses are of considerable importance, especially at dehydrating conditions. Given that ohmic losses are considerably reduced when using thin membranes and cathode electrodes (Figs. 1 and 2), temperature distributions at different hydrating conditions (50 and 100% RH) are assumed to be similar for systems with low ohmic losses.

3.6. Comparison to experimental data

Data validation is an important aspect of every work concerning numerical simulation. Therefore comparisons between experimental and numerical distributions become of high importance not only to confirm the suitability of the numerical data, but also to improve the understanding of different important phenomenon that may take place in the control volume. Up to now, some experimental setup [32–36] have been developed to get approaches of current density distributions in PEMFC, which are important advances, given that the polarization curves may be misleading for data validation [14]. In this work, some of data of Mench et al. [37] is used to show the suitability of this model to study the behaviors of PEMFC (Fig. 11) over a wide range of current densities. The numerical input data was adjusted to the experimental conditions of Ref. [37] in order to achieve a reliable validation. Results show that the numerical current density distributions show a reasonable increase when lowering the cell potential and working under mass transport limitations (oxygen depletion). This behavior is in agreement with the experimental data presented in Ref. [37], consequently this modeling proves to be sensitive to different factors that may govern the performance of PEMFC.

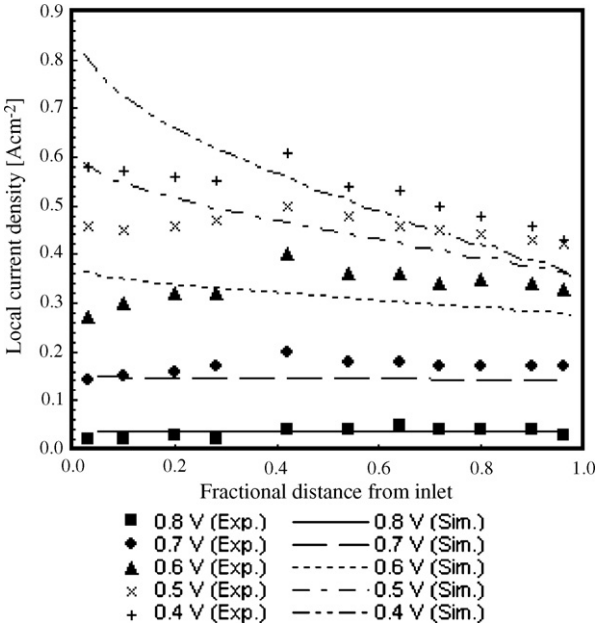

Fig. 11. Comparison between numerical and experimental [37] current density distributions.

4. Conclusions

Results showed that geometrical parameters may have an important influence on PEMFC performance under conditions arbitrarily chosen in this work. This work also showed the importance of simultaneously calculating water absorption and desorption by polymer electrolyte and water saturation, in order to establish actual ohmic and concentration losses under different hydrating conditions.

Polymer membrane may cause serious ohmic losses if thickness is high. Use of thin polymer membrane considerably enhances PEMFC power by reducing ohmic losses, especially under dehydrating conditions.

PEMFC power may be improved by using thin cathode catalyst layers. Proton resistance to active sites is small; consequently cathode reaction rate is not affected by activation losses. Not only ohmic losses may be enhanced but also concentration losses. Concentration of platinum particles becomes higher, and so reactants transfer control may be reduced. Therefore cathode catalyst layer thickness plays an important role when optimizing electrochemical parameters.

Permeability of the gas diffusion layer is an important factor to control the liquid saturation. In numerical terms, high permeabilities (greater than 1e−15 m^2) could enhance disposal of liquid water in the gas diffusion layer, keeping the saturation in porous mediums controlled (less than 0.2).

Wide gas channels yield lower concentration losses under fully humidifying conditions, and as such better performance is achieved under these conditions at high current densities. However, ribs width should be wide enough to avoid ohmic losses by electron transport from anode to cathode.

Temperature gradients could be important when current density causes high ohmic losses. Otherwise, the system could be treated as isothermal under the electrochemical and geometrical conditions of this work.

Effect of the humidity over PEMFC power density could be considerably diminished if using the optimal geometrical parameters to minimize ohmic and concentration losses. Operation at 50% RH showed to be satisfactory when using polymer membranes thinner than 50 μm. In the case of catalyst layers, PEMFC performance is likely to become independent of this factor if using a thickness thinner than 6.25 μm even at dehydrating conditions like 50% RH.

References

[1] S. Um, C.Y. Wang, K.S. Chen, J. Electrochem. Soc. 147 (12) (2000) 4485–4493.
[2] S. Dutta, S. Shimpalee, J.W. Van Zee, J. Appl. Electrochem. 30 (2000) 35–146.
[3] Z.H. Wang, C.Y. Wang, K.S. Chen, J. Power Sources 94 (2001) 40–50.
[4] D. Natarajan, T. Van Nguyen, J. Electrochem. Soc. 148 (12) (2001) A1324–A1335.
[5] T. Berning, D.M. Lu, N. Djilali, J. Power Sources 106 (2002) 284–294.
[6] T. Berning, N. Djilali, J. Electrochem. Soc. 150 (12) (2003) A1589–A1598.
[7] J.H. Nam, M. Kaviany, Int. J. Heat Mass Transfer 46 (2003) 4595–4611.
[8] S. Um, C.Y. Wang, J. Power Sources 125 (2004) 40–51.
[9] H. Meng, C.Y. Wang, Chem. Eng. Sci. 59 (2004) 3331–3343.

[10] U. Pasaogullari, C.-Y. Wang, J. Electrochem. Soc. 152 (2) (2005) A380–A390.
[11] H. Wang, C.Y. Wang, J. Electrochem. Soc. 152 (9) (2005) A1733–A1741.
[12] G. Guvelioglu, H. Stenger, J. Power Sources 147 (2005) 95–106.
[13] K. Lum, J. McGuirk, J. Power Sources 143 (2004) 103–124.
[14] C.-Y. Wang, Chem. Rev. 104 (10) (2004) 4727–4766.
[15] L. Matamoros, D. Brüggemann, J. Power Sources 161 (2006) 203–213.
[16] T.E. Springer, T.A. Zawodzinski, S. Gottesfeld, J. Electrochem. Soc. 138 (8) (1991) 2334–2342.
[17] J.T. Hinatsu, M. Mizuhata, H. Takenata, J. Electrochem. Sources 141 (6) (1994) 1493–1498.
[18] Y. Wang, C.-Y. Wang, J. Electrochem. Soc. 152 (2) (2005) A445–A453.
[19] V. Gurau, H. Liu, S. Kakac, AIChE J. 44 (1998) 2410–2422.
[20] M. Lampinen, M. Fomino, J. Electrochem. Soc. 140 (12) (1993) 3537–3546.
[21] K. Broka, P. Ekdunge, J. Appl. Electrochem. 27 (1997) 281–289.
[22] M.L. Perry, J. Newman, E.J. Cairns, J. Electrochem. Soc. 145 (1) (1998) 5–15.
[23] C. Marr, X. Li, J. Power Sources 77 (1999) 17–27.
[24] F. Jaouen, G. Lindbergh, G. Sundholm, J. Electrochem. Soc. 149 (4) (2002) A437–A447.
[25] Q. Wang, D. Song, T. Navessin, S. Holdcroft, Z. Liu, Electrochim. Acta 50 (2004) 725–730.
[26] D.M. Bernardi, M.W. Verbrugge, J. Electrochem. Soc. 139 (9) (1992) 2477–2491.
[27] A. Parthasarathy, S. Srinivasan, J. Appleby, J. Electrochem. Soc. 139 (9) (1992) A437–A447.
[28] M.M. Tomadakis, S.V. Sotirchos, AIChE J. 39 (1993) 397–412.
[29] R.B. Bird, W.E. Stewart, E.N. Lightfoot, Transport Phenomena, Wiley, New York, 1960.
[30] W. Neubrand, Dissertation, Universität Stuttgart, Germany, 1999.
[31] T.A. Zawodzinski, C. Derouin, S. Radzinski, R. Sherman, V.T. Smith, T. Springer, S. Gottesfeld, J. Electrochem. Soc. 140 (4) (1993) 1041–1047.
[32] J. Stumper, S. Campell, D. Wilkinson, M. Johnson, M. Davis, Electrochim. Acta 43 (1998) 3773.
[33] S. Cleghorn, C. Derouin, M. Wilson, S. Gottesfeld, J. Appl. Electrochem. 28 (2000) 663.
[34] C. Wieser, A. Helmbold, E. Guelzow, J. Appl. Electrochem. 30 (2000) 803.
[35] M. Noponen, T. Mennola, M. Mikkola, T. Hottinen, P. Lund, J. Power Sources 106 (2002) 304.
[36] M.M. Mench, C.Y. Wang, J. Electrochem. Soc. 150 (2003) A79.
[37] M.M. Mench, C.Y. Wang, M. Ishikawa, J. Electrochem. Soc. 150 (8) (2003) A1052–A1059.